(3+1)D Event-by-event Pre-equilibrium Dynamics in Heavy-ion Collisions

Jie Zhu

In collaboration with Xiaojian Du and Sören Schlichting

Phys. Rev. D 113, 096009 (2026)

August 17, 2026, Helsinki

17–21 Aug 2026
Helsinki, Finland
Strong and Electro-Weak Matter 2026

UNIVERSITÄT BIELEFELD

CRC–TR 211
Strong-interaction matter under extreme conditions

Contents

Motivation: longitudinal structure of HIC

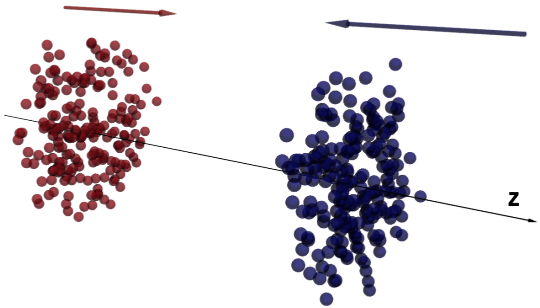

Longitudinally boost-invariant

$$\eta_s = \frac{1}{2}\ln\frac{t+z}{t-z} = 0$$

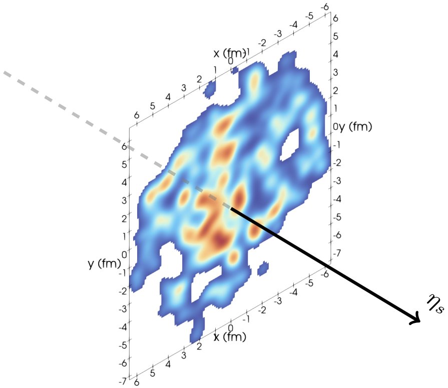

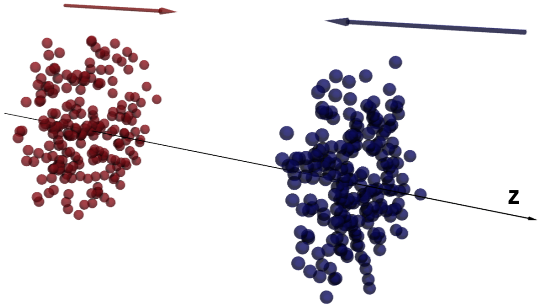

Longitudinally boost-invariant

$$\eta_s = \frac{1}{2}\ln\frac{t+z}{t-z} = 0$$

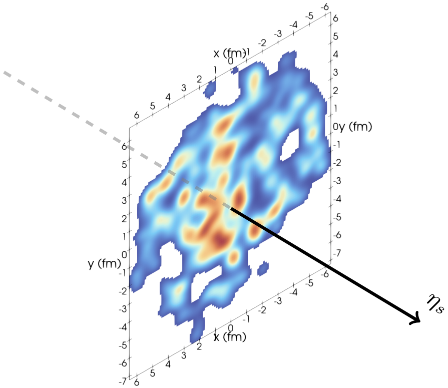

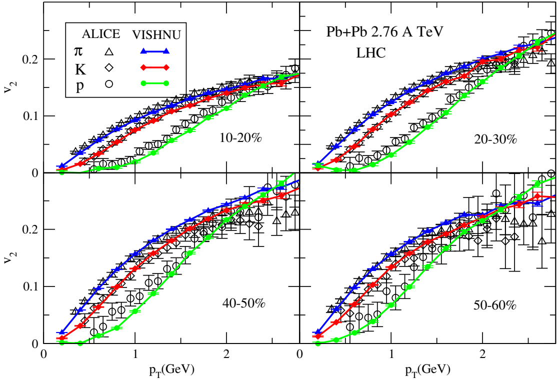

Strong and Electro-Weak Matter 2026

$$\eta_s = \frac{1}{2}\ln\frac{t+z}{t-z}$$

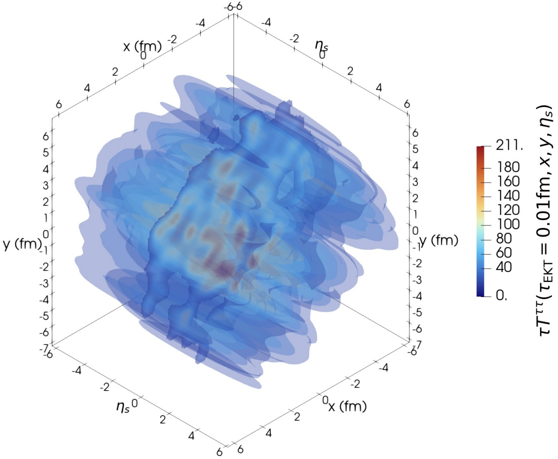

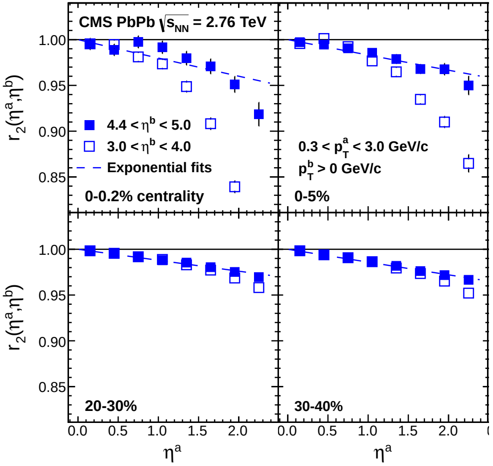

- Call for full (3+1)D simulations of HICs.

Strong and Electro-Weak Matter 2026

17–21 Aug 2026 Helsinki, Finland

$$\eta_s = \frac{1}{2}\ln\frac{t+z}{t-z}$$

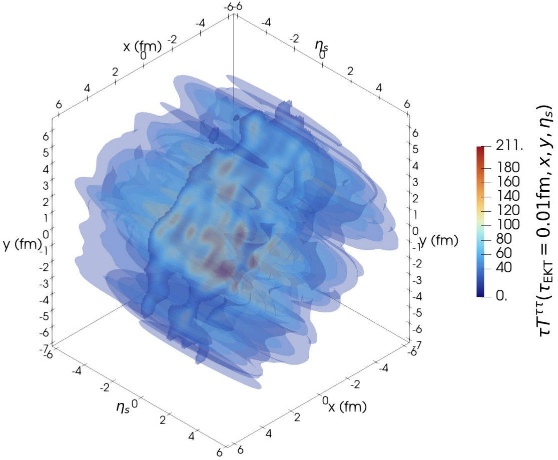

- Longitudinal structure in initial state
  - IP-Glasma-3D
  - AMPT: 3D transport model
  - T$_\mathrm{R}$ENTo-3D
- Pre-equilibrium dynamics
  - KøMPøST in 2D
- Longitudinal late time dynamics
  - (3+1)D hydrodynamics
  - Afterburner

Pre-equilibrium evolution: from the view of KøMPøST

- Propagation of the non-equilibrium $T^{\mu\nu}$ from an initial time τ_{EKT} to a time τ_{hydro} when hydrodynamics becomes applicable.

$$T^{\mu\nu}\left(\tau_{\mathsf{EKT}}, \mathbf{x}\right)\Big|_{\text{out-of-equilibrium}} \longrightarrow T^{\mu\nu}\left(\tau_{\mathsf{hydro}}, \mathbf{x}\right). \qquad (1)$$

- All contributions to $T^{\mu\nu}$ at $\left(\tau_{\mathsf{hydro}}, \mathbf{x}\right)$ are determined by the initial conditions at earlier time τ_{EKT} in causal neighborhood of point $\mathbf{x}$.

$$\left|\mathbf{x}' - \mathbf{x}\right| < c\left(\tau_{\mathsf{hydro}} - \tau_{\mathsf{EKT}}\right). \qquad (2)$$

- The fluctuations of $T^{\mu\nu}$ within causal circle that we need to consider are small in large collision systems.
  - The long wavelength variations of $T^{\mu\nu}$ within the causal circle are small, due to $\left(\tau_{\mathsf{hydro}} - \tau_{\mathsf{EKT}}\right)/R_{\mathrm{Pb}} \ll 1$.
  - Short wavelength fluctuations (of order nucleon size or less) are washed out.

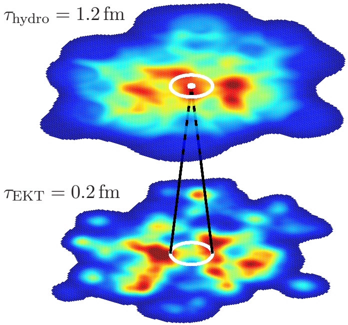

PRL 122, 122302 (2019)

Strategy of KøMPøST

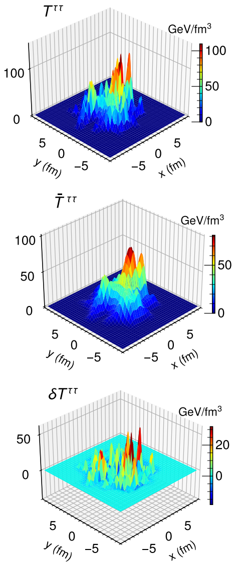

- $T^{\mu\nu}(\tau, \mathbf{x})$ can be expressed as a sum of the evolved background and the response to the initial out-of-equilibrium perturbations,

$$T^{\mu\nu}(\tau, \mathbf{x}) = \bar{T}^{\mu\nu}_{\mathbf{x}}(\tau) + \delta T^{\mu\nu}_{\mathbf{x}}(\tau). \tag{3}$$

- The non-equilibrium background ($\bar{T}^{\mu\nu}$) evolution is described by a universal function $\mathcal{E}\left[x = \frac{\tau T_{\mathrm{id.}}}{\eta/s}\right]$ derived from the scaling behavior of kinetic evolution.

$$\bar{T}^{\mu\nu} = \mathrm{diag}\left(e, P_T, P_T, \frac{1}{\tau^2} P_L\right), \qquad e = \nu_g \frac{\pi^2}{30} T^4_{\mathrm{id.}} \mathcal{E}\left[x = \frac{\tau T_{\mathrm{id.}}}{\eta/s}\right]. \tag{4}$$

- Perturbations around the background can be described by **linear response theory**,

$$\frac{\delta T^{\mu\nu}(\tau, \mathbf{x})}{\bar{T}^{\tau\tau}_{\mathbf{x}}(\tau)} = \int d^2\mathbf{x}_0 \; G^{\mu\nu}_{\alpha\beta}(\mathbf{x}, \mathbf{x}_0, \tau, \tau_0) \frac{\delta T^{\alpha\beta}_{\mathbf{x}}(\tau_0, \mathbf{x}_0)}{\bar{T}^{\tau\tau}_{\mathbf{x}}(\tau_0)}. \tag{5}$$

KøMPøST $\Longrightarrow$ KøMPøST-3D

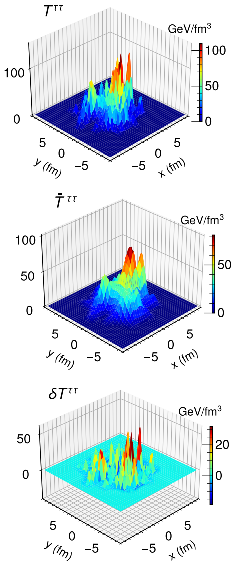

- $T^{\mu\nu}(\tau, \mathbf{x})$ can be expressed as a sum of the evolved background and the response to the initial out-of-equilibrium perturbations,

$$T^{\mu\nu}(\tau, \mathbf{x}) = \bar{T}^{\mu\nu}_{\mathbf{x}}(\tau) + \delta T^{\mu\nu}_{\mathbf{x}}(\tau). \tag{6}$$

- The non-equilibrium background ($\bar{T}^{\mu\nu}$) evolution is described by a universal function $\mathcal{E}\left[x = \frac{\tau T_{\mathrm{id.}}}{\eta/s}\right]$ derived from the scaling behavior of kinetic evolution.

$$\bar{T}^{\mu\nu} = \mathrm{diag}\left(e, P_T, P_T, \frac{1}{\tau^2}P_L\right), \qquad e = \nu_g \frac{\pi^2}{30} T^4_{\mathrm{id.}} \mathcal{E}\left[x = \frac{\tau T_{\mathrm{id.}}}{\eta/s}\right]. \tag{7}$$

- Perturbations around the background can be described by **linear response theory**,

$$\frac{\delta T^{\mu\nu}(\tau, \mathbf{x}, \eta)}{\overline{T}^{\tau\tau}_{\mathbf{x},\eta}(\tau)} = \int d^2\mathbf{x}_0\, d\eta_0 G^{\mu\nu}_{\alpha\beta}(\mathbf{x}, \eta, \mathbf{x}_0, \eta_0, \tau, \tau_0) \frac{\delta T^{\alpha\beta}_{\mathbf{x},\eta}(\tau_0, \mathbf{x}_0, \eta_0)}{\overline{T}^{\tau\tau}_{\mathbf{x},\eta}(\tau_0)}. \tag{8}$$

- Boltzmann equation under relaxation time approximation.

$$\left[p^\tau \partial_\tau + p^i \partial_i - \frac{p_\eta}{\tau^2}\partial_\eta\right] f(x,p) = -\frac{p_\mu u^\mu(x)}{\tau_R}\left[f(x,p) - f_{eq}\left(p_\mu \beta^\mu(x)\right)\right]. \tag{9}$$

- Decompose distribution function into background and perturbation

$$f(x,p) = f_{BG}(x,p) + \delta f(x,p). \tag{10}$$

- Utilize the method of moments to transform PDE to a set of coupled ODEs. PRD 102, 056003 (2020)

Energy response:

$$\delta T^{\tau\tau}(\tau_{\text{EKT}}) \to \delta T^{\tau\tau}(\tau)$$

Def: scaled time var, $\tilde{\omega} \equiv \frac{\tau T_{\text{id}}}{4\pi\eta/s}$

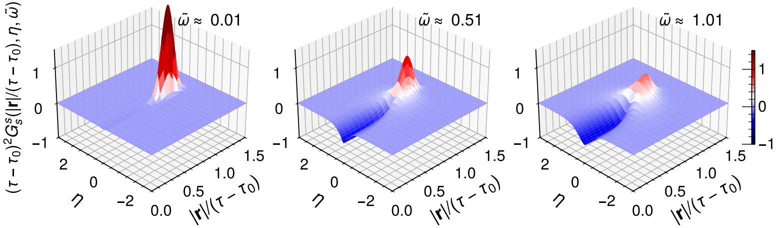

3D distribution $\tau T^{\tau\mu}(x, y, \eta_s)$

McDipper → KøMPøST-3D → CLVisc $\xrightarrow{\text{Cooper-Frye}}$ SMASH

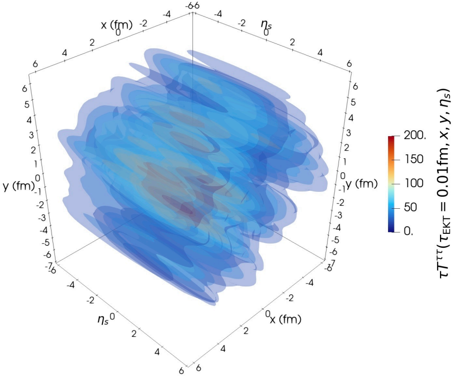

$\Longrightarrow$

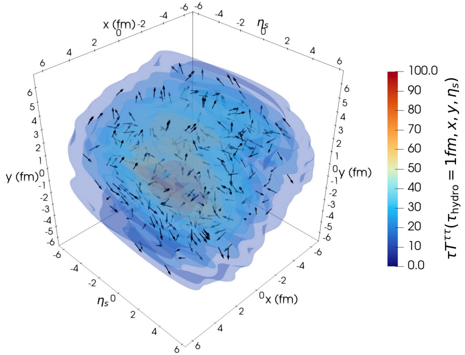

- 3D energy profile $\tau T^{\tau\tau}(x, y, \eta_s)$ from McDipper initial state model is evolved with KøMPøST-3D from $\tau_{\rm EKT} = 0.01$ fm to $\tau_{\rm hydro} = 1.0$ fm.

PRC 109, 044916 (2024) PRC 97, 064918 (2018); PRC 105, 034909 (2022) PRC 94, 054905 (2016); JHEP 05, 026 (2006)

Averaged hydrodynamic fields

KøMPøST-3D provides a smooth transition from 3D out-of-equilibrium initial conditions to (3+1)D near-equilibrium viscous hydrodynamics.

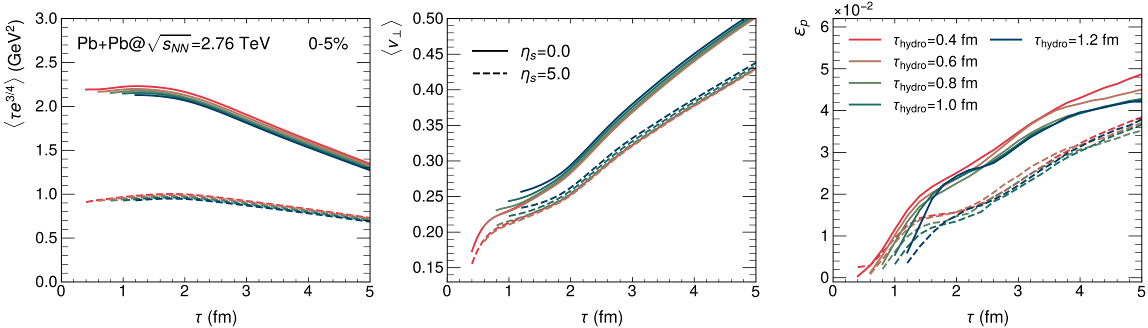

- The evolution of energy density and radial flow at midrapidity and forward rapidity shows only weak sensitivity to τ_{hydro}; the small differences mainly originate from the mismatch in the EoS.
- Time evolution of the momentum eccentricity ε_p shows an evident dependence on hydro starting time for both midrapidity and forward rapidity.

Hadronic observables

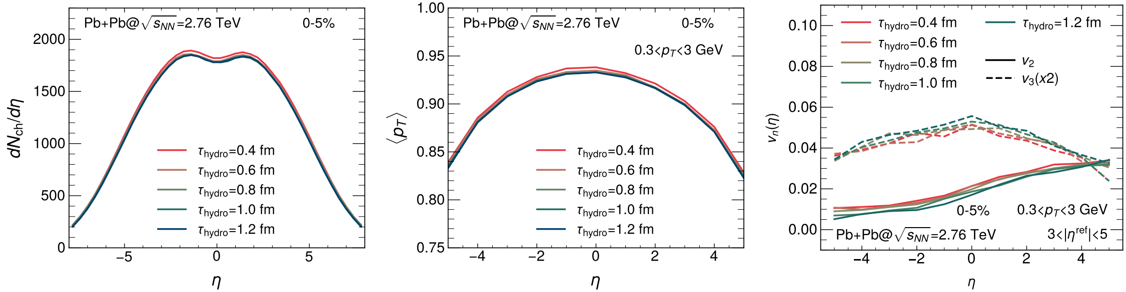

- The rapidity distributions of charged-hadron multiplicity and mean transverse momentum are only weakly sensitive to τ_{hydro}.
- The η-differential anisotropic flow coefficients exhibit a systematic, though modest, sensitivity to τ_{hydro}, mainly due to the insufficient buildup of the momentum anisotropy ε_p during the pre-equilibrium stage.

Summary and outlook

Summary

- A preliminary attempt for constructing a 3D framework, KøMPøST-3D, to describe the preequilibrium dynamics of HICs was made.
- The hydrodynamization can be achieved in most of the collision area not only in transverse plane but also in longitudinal direction.
- The longitudinal structure of $dN/d\eta$, $\langle p_T \rangle$ and $v_{2,3}(\eta)$ show little sensitivity to τ_{hydro} which means KøMPøST-3D provides a smooth transition from initial conditions to viscous hydrodynamics.

Future Plans and Improvements

- A more realistic input of response functions from QCD kinetic theory.
- The response to initial energy $\delta T^{\tau\tau}$, momentum $(\delta T^{\tau i})$ and tensor perturbations (δT^{ij}) for a comprehensive propagation of the information from initial conditions.

Summary and outlook

Summary

- A preliminary attempt for constructing a 3D framework, KøMPøST-3D, to describe the preequilibrium dynamics of HICs was made.
- The hydrodynamization can be achieved in most of the collision area not only in transverse plane but also in longitudinal direction.
- The longitudinal structure of $dN/d\eta$, $\langle p_T \rangle$ and $v_{2,3}(\eta)$ show little sensitivity to τ_{hydro} which means KøMPøST-3D provides a smooth transition from initial conditions to viscous hydrodynamics.

Future Plans and Improvements

- A more realistic input of response functions from QCD kinetic theory.
- The response to initial energy $\delta T^{\tau\tau}$, momentum $(\delta T^{\tau i})$ and tensor perturbations (δT^{ij}) for a comprehensive propagation of the information from initial conditions.

Thank you for your attention!

Appendix

Time evolution of the energy density $\tau\varepsilon(x, y, \eta_s)$

- We can see the smearing of energy profile both in transverse plane and reaction plane.

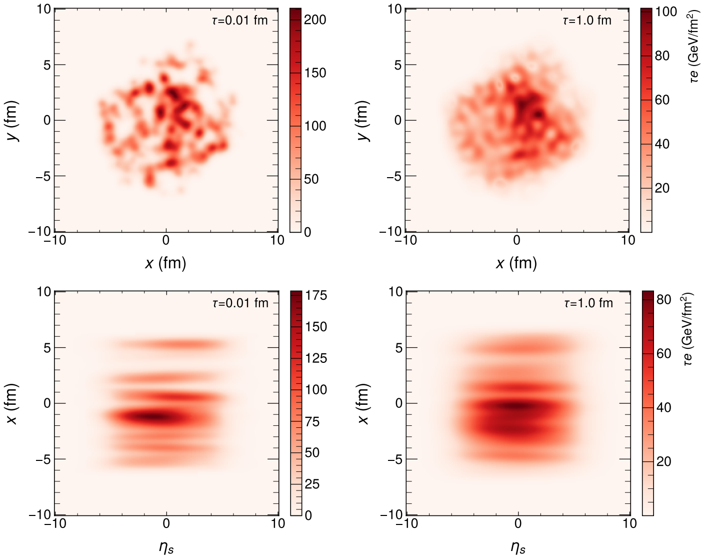

Hydrodynamization

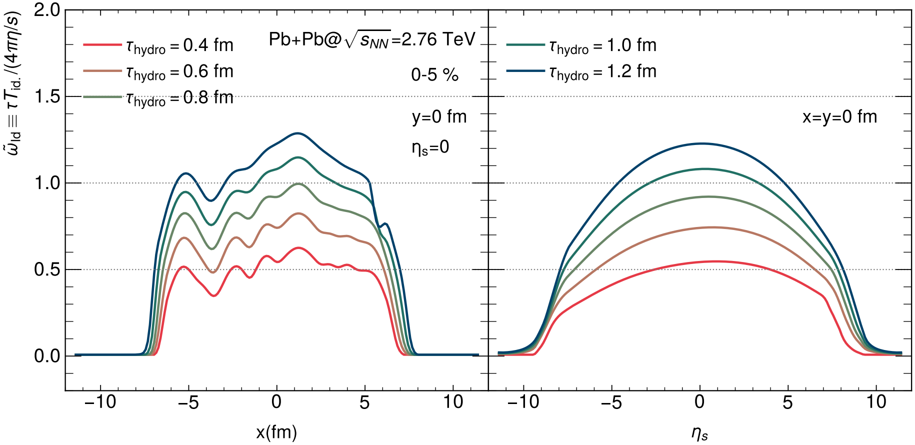

- Values of $\tau T_{\rm id}/(4\pi\eta/s) > 1$ indicate that the system can be described by hydrodynamics.
- Since the local energy density at the edges is significantly smaller, the edges of the fireball remain at $\tau T_{\rm id}/(4\pi\eta/s) < 1$ for a longer time.

RTA VS QCD

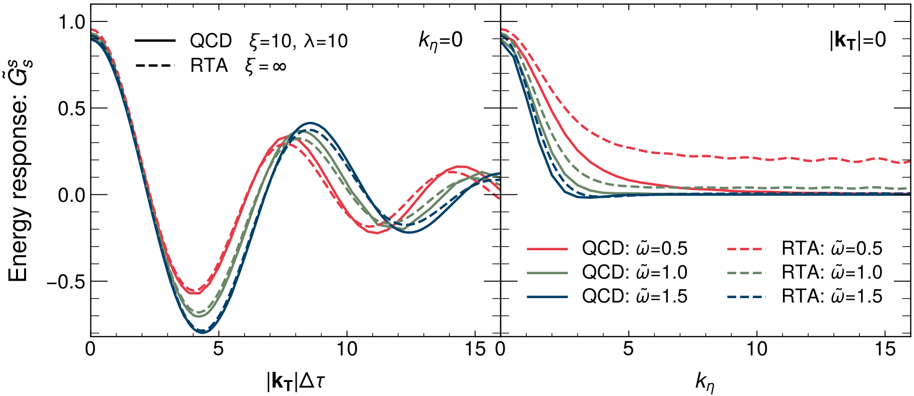

- The deviation of RTA from the realistic QCD simulations is sizeable at early times and high wavenumbers because the initial distributions in QCD and RTA are chosen differently.
- The difference becomes negligibly small at sufficiently late times and in the low-wavenumber (long-wavelength) region.

Numerical solution to RTA

Utilize method of moments to transform PDE to set of coupled ODEs.

- Moments of background:

PRD 102, 056003 (2020); S. Ochsenfeld, Master's thesis, 2020

$$E_l^m(\tau) = \nu_{eff} \int \frac{dp_\eta}{2\pi} \int \frac{d^2\mathbf{p_T}}{(2\pi)^2} \tau^{1/3} p^\tau Y_l^m \left(\phi_{\mathbf{p_T}}, \theta_\eta\right) f_{BG}\left(\tau, p_T, |p_\eta|\right). \quad (11)$$

- Respective moments of perturbations:

$$\delta E_{l,k}^m(\tau) = \int \frac{dp_\eta}{2\pi} \int \frac{d^2\mathbf{p_T}}{(2\pi)^2} \tau^{1/3} p^\tau Y_l^m \left(\phi_{\mathbf{p_T k_T}}, \theta_\eta\right) \delta f_k\left(\tau, \mathbf{p_T}, p_\eta\right). \quad (12)$$

- Specify an initial condition to particle distribution function.

$$\begin{aligned} f_{BG}\left(\tau_0, p_T, p_\eta\right) &= \frac{(2\pi)^3}{\nu_{\text{eff}}} \delta\left(p_\eta\right) \frac{\mathrm{d}N_0}{\mathrm{d}\eta\ \mathrm{d}^2\mathbf{p_T}\mathrm{d}^2\mathbf{x}}, \\ \delta f_k\left(\tau_0, \mathbf{p_T}, p_\eta\right) &= -\left(\frac{|\mathbf{p_T}|}{3} \partial_{|\mathbf{p_T}|} f_{BG}^{(0)}\left(|\mathbf{p_T}|, p_\eta\right)\right) e^{-i\left(\frac{\mathbf{p_T}\cdot\mathbf{k_T}}{|\mathbf{p_T}|}\tau_0 - k_\eta \operatorname{arcsch}\left(\frac{\mathbf{p_T}\tau_0}{p_\eta}\right)\right)}. \end{aligned} \quad (13)$$

- Runge-Kutta scheme of fourth order is used to solve moments evolution.

Under RTA, Boltzmann equation is simplified to

$$\left[p^\tau\partial_\tau + p^i\partial_i - \frac{p_\eta}{\tau^2}\partial_\eta\right] f(x,p) = -\frac{p_\mu u^\mu(x)}{\tau_R}\left[f(x,p) - f_{eq}\left(p_\mu\beta^\mu(x)\right)\right]. \tag{14}$$

- Decomposition of distribution function:

$$f(x,p) = f_{BG}(x,p) + \delta f(x,p). \tag{15}$$

- Longitudinally boost invariant and locally homogeneous in the transverse plane background:

$$\tau\partial_\tau f_{BG}\left(\tau, p_T, |p_\eta|\right) = -\frac{\tau}{\tau_R}\left[f_{BG}\left(\tau, p_T, |p_\eta|\right) - f_{eq}\left(\frac{p^\tau}{T(\tau)}\right)\right]. \tag{16}$$

- Deviations from this behavior can be studied by applying small fluctuations on top of this background. After linearization it yields

$$p^\mu\partial_\mu\delta f = -\frac{p^\tau}{\tau_R}\delta f + \frac{p_\mu\delta u^\mu}{\tau_R}\left[(f_{eq} - f_{BG}) + \frac{p^\tau}{T}f'_{eq}\right] - \frac{p^\tau}{\tau_R}\delta T\left[\frac{1}{\tau_R}\frac{\partial\tau_R}{\partial T}(f_{eq} - f_{BG}) + \frac{p^\tau}{T^2}f'_{eq}\right]. \tag{17}$$

Decomposition of response functions

In momentum space, the response functions for (scalar) energy perturbations are decomposed as follows:

$$
\begin{aligned}
\tilde{G}^{\tau\tau}_{\tau\tau}(\mathbf{k_T}, k_\eta) &= \tilde{G}^{s}_{s}(|\mathbf{k_T}|, |k_\eta|) \\
\tilde{G}^{\tau i}_{\tau\tau}(\mathbf{k_T}, k_\eta) &= -i\tilde{G}^{v}_{s}(|\mathbf{k_T}|, |k_\eta|)\frac{\mathbf{k_T}^{i}}{|\mathbf{k_T}|} \\
\tilde{G}^{ij}_{\tau\tau}(\mathbf{k_T}, k_\eta) &= \tilde{G}^{t,\delta}_{s}(|\mathbf{k_T}|, |k_\eta|)\delta^{ij} + \tilde{G}^{t,k}_{s}(|\mathbf{k_T}|, |k_\eta|)\frac{\mathbf{k_T}^{i}\mathbf{k_T}^{j}}{|\mathbf{k_T}|^2} \\
\tilde{G}^{\eta\eta}_{\tau\tau}\left(\mathbf{k_T}, k_\eta\right) &= \tilde{G}^{\eta}_{s}\left(|\mathbf{k_T}|, |k_\eta|\right) \\
\tilde{G}^{\tau\eta}_{\tau\tau}\left(\mathbf{k_T}, k_\eta\right) &= -i\frac{k_\eta}{\left|k_\eta\right|}\tilde{G}^{s,\eta}_{s}\left(|\mathbf{k_T}|, |k_\eta|\right) \\
\tilde{G}^{i\eta}_{\tau\tau}\left(\mathbf{k_T}, k_\eta\right) &= \frac{k^{i}_{T}k_\eta}{|\mathbf{k_T}|\left|k_\eta\right|}\tilde{G}^{v,\eta}_{s}\left(|\mathbf{k_T}|, |k_\eta|\right)
\end{aligned}
\tag{18}
$$

In coordinate space, the decomposion for energy perturbations takes the following form

$$
\begin{aligned}
G^{\tau\tau}_{\tau\tau}(\mathbf{r},\eta) &= G^{s}_{s}\left(|\mathbf{r}|,|\eta|\right)\\
G^{\tau i}_{\tau\tau}(\mathbf{r},\eta) &= \frac{\mathbf{r}^i}{|\mathbf{r}|}G^{v}_{s}\left(|\mathbf{r}|,|\eta|\right)\\
G^{ij}_{\tau\tau}(\mathbf{r},\eta) &= G^{t,\delta}_{s}\left(|\mathbf{r}|,|\eta|\right)\delta^{ij} + G^{t,r}_{s}\left(|\mathbf{r}|,|\eta|\right)\frac{\mathbf{r}^i\mathbf{r}^j}{|\mathbf{r}|^2}\\
G^{\eta\eta}_{\tau\tau}(\mathbf{r},\eta) &= G^{\eta}_{s}\left(|\mathbf{r}|,|\eta|\right)\\
G^{\tau\eta}_{\tau\tau}(\mathbf{r},\eta) &= \frac{\eta}{|\eta|}G^{s,\eta}_{s}\left(|\mathbf{r}|,|\eta|\right)\\
G^{i\eta}_{\tau\tau}(\mathbf{r},\eta) &= \frac{\mathbf{r}^i\eta}{|\mathbf{r}||\eta|}G^{v,\eta}_{s}(|\mathbf{r}|,|\eta|)
\end{aligned}
\tag{19}
$$

Reverse Fourier transformation of response functions

Strong and Electro-Weak Matter 2026

The coordinate space Green functions are related to their momentum space counterparts according to the Fourier-Hankel transformation, for energy perturbation,

$$G_s^s\left(|\mathbf{r}|,|\eta|\right)=\frac{1}{2\pi^2}\int_0^\infty d|\mathbf{k_T}||\mathbf{k_T}|dk_\eta\cos(k_\eta\cdot\eta)J_0(|\mathbf{k_T}||\mathbf{r}|)\tilde{G}_s^s\left(|\mathbf{k_T}|,|k_\eta|\right)$$

$$G_s^v\left(|\mathbf{r}|,|\eta|\right)=\frac{1}{2\pi^2}\int_0^\infty d|\mathbf{k_T}||\mathbf{k_T}|dk_\eta\cos(k_\eta\cdot\eta)J_1(|\mathbf{k_T}||\mathbf{r}|)\tilde{G}_s^v\left(|\mathbf{k_T}|,|k_\eta|\right)$$

$$G_s^{t,\delta}\left(|\mathbf{r}|,|\eta|\right)=\frac{1}{2\pi^2}\int_0^\infty d|\mathbf{k_T}||\mathbf{k_T}|dk_\eta\cos(k_\eta\cdot\eta)\left[J_0(|\mathbf{k_T}||\mathbf{r}|)\tilde{G}_s^{t,\delta}\left(|\mathbf{k_T}|,|k_\eta|\right)+\frac{J_1(|\mathbf{k_T}||\mathbf{r}|)}{|\mathbf{k_T}||\mathbf{r}|}\tilde{G}_s^{t,k}\left(|\mathbf{k_T}|,|k_\eta|\right)\right]$$

$$G_s^{t,r}\left(|\mathbf{r}|,|\eta|\right)=\frac{-1}{2\pi^2}\int_0^\infty d|\mathbf{k_T}||\mathbf{k_T}|dk_\eta\cos(k_\eta\cdot\eta)J_2(|\mathbf{k_T}||\mathbf{r}|)\tilde{G}_s^{t,k}\left(|\mathbf{k_T}|,|k_\eta|\right)$$

$$G_s^\eta(|\mathbf{r}|,|\eta|)=\frac{1}{2\pi^2}\int_0^\infty d|\mathbf{k_T}||\mathbf{k_T}|dk_\eta\cos(k_\eta\cdot\eta)J_0(|\mathbf{k_T}||\mathbf{r}|)\tilde{G}_s^\eta\left(|\mathbf{k_T}|,|k_\eta|\right)$$

$$G_s^{s,\eta}(|\mathbf{r}|,|\eta|)=\frac{\eta}{2\pi^2|\eta|}\int_0^\infty d|\mathbf{k_T}||\mathbf{k_T}|dk_\eta\sin(k_\eta\cdot\eta)J_0(|\mathbf{k_T}||\mathbf{r}|)\tilde{G}_s^{s,\eta}\left(|\mathbf{k_T}|,|k_\eta|\right)$$

$$G_s^{v,\eta}(|\mathbf{r}|,|\eta|)=\frac{-\eta}{2\pi^2|\eta|}\int_0^\infty d|\mathbf{k_T}||\mathbf{k_T}|dk_\eta\sin(k_\eta\cdot\eta)J_1(|\mathbf{k_T}||\mathbf{r}|)\tilde{G}_s^{v,\eta}\left(|\mathbf{k_T}|,|k_\eta|\right)$$

- Extra smearing kernels "$\exp(-\sigma^2|\mathbf{k_T}|^2/2)\ \exp(-\sigma_\eta^2|\mathbf{k}_\eta|^2/2)$" are implemented during transformation. In this work, we take $\sigma=0.1,\sigma_\eta=0.1$.

Constitutive relations

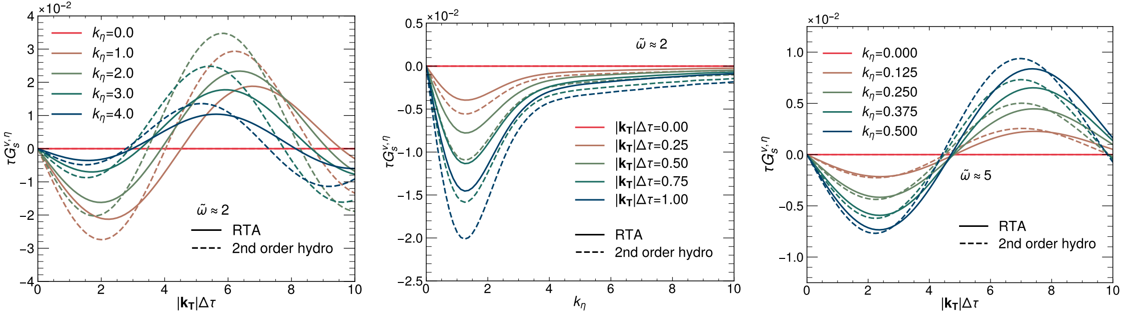

Comparison of the response functions for δT from an initial energy perturbation with the constitutive relations of second order hydrodynamics.

$$\tilde{G}_s^{v,\eta}(\tau,\tau_0,|\mathbf{k}|,|k^\eta|) = \left(\eta\tau_\pi \frac{c_s^2+1/3}{\tau} - \eta - \frac{4\lambda_1}{3\tau}\right)\left(\frac{|\mathbf{k}|\tilde{G}_s^{s,\eta}(\tau,\tau_0,|\mathbf{k}|,|k^\eta|)}{\bar{T}^{\tau\tau}+\bar{T}^\eta_\eta} + \frac{|k^\eta|\tilde{G}_s^{v}(\tau,\tau_0,|\mathbf{k}|,|k^\eta|)}{\bar{T}^{\tau\tau}+\frac{1}{2}\bar{T}^k_k}\right) \quad (20)$$

Practical implementation of KøMPøST-3D

- Background:

$$\bar{T}^{\tau\tau}_{\mathbf{x}_0,\eta_0}(\tau) \equiv \int d^2\mathbf{x}' d\eta' \frac{1}{2\pi\sigma^2_{\mathrm{BG}}} e^{\frac{-\left(\mathbf{x}'-\mathbf{x}_0\right)^2}{2\sigma^2_{\mathrm{BG}}}} \frac{1}{\sqrt{2\pi\sigma^2_{\mathrm{BG},\eta}}} e^{\frac{-\left(\eta'-\eta_0\right)^2}{2\sigma^2_{\mathrm{BG},\eta}}} T^{\tau\tau}\left(\tau, \mathbf{x}', \eta'\right) \tag{21}$$

  where $\sigma_{\mathrm{BG}} = \Delta\tau/2$, $\sigma_{\mathrm{BG},\eta} = 3/2$, $\Delta\tau = \tau_{hydro} - \tau_{EKT}$
- First we build the background by the above equation for each point. The integration was done in "causal area" [-4$\sqrt{2}\sigma_{\mathrm{BG}}$, 4$\sqrt{2}\sigma_{\mathrm{BG}}$] and [-4$\sqrt{2}\sigma_{\mathrm{BG},\eta}$, 4$\sqrt{2}\sigma_{\mathrm{BG},\eta}$]
- Then at each point, we also integrate the response of peturbations inside the "causal area" $\Delta|\mathbf{r}| < \Delta\tau + 0.3$ and $\Delta\eta < 3$(from RTA dynamics.)

(3+1)D CLVisc viscous hydrodynamics

The (3+1)D CLVisc hydrodynamics model is used to simulate the space-time evolution of the QGP fireball.[PRC 105, 034909 (2022), PRC 97, 064918 (2018)

- Energy-momentum and baryon number conservation equations

$$\partial_\mu T^{\mu\nu} = 0 \tag{22}$$

- Solve the evolution equations of $\pi^{\mu\nu}$using the Israel-Stewart-like equations [PRC 98, 034916 (2018)]

$$\tau_\pi \Delta^{\mu\nu}_{\alpha\beta} D\pi^{\alpha\beta} + \pi^{\mu\nu} = \eta_v \sigma^{\mu\nu} - \delta_{\pi\pi}\pi^{\mu\nu}\theta - \tau_{\pi\pi}\pi^{\lambda\langle\mu}\sigma^{\nu\rangle}_{\lambda} + \varphi_1 \pi^{\langle\mu}_{\alpha}\pi^{\nu\rangle\alpha} \tag{23}$$

- Sample thermal hadrons using the Cooper-Frye prescription,

$$\frac{dN_i}{dY p_T dp_T d\phi} = \frac{g_i}{(2\pi)^3} \int_\Sigma p^\mu d\Sigma_\mu f_{\rm eq}(1+\delta f_\pi). \tag{24}$$

- Thermal equilibrium term $f_{\rm eq}$ and out-of-equilibrium correction δf are given as,

$$\begin{aligned} f_{\rm eq} &= \frac{1}{\exp\left[\left(p\cdot u - B\mu_B\right)/T\right] \pm 1}, \\ \delta f_\pi &= (1 \pm f_{\rm eq}) \frac{p_\mu p_\nu \pi^{\mu\nu}}{2T^2(e+P)}. \end{aligned} \tag{25}$$

- After the thermal hadrons are produced, a hadronic afterburner can be employed to simulate interactions betweem them. (Or they are forced to decay into stable particles immediately.)